Article

Producing Energy-Rich Microalgae Biomass for Liquid Biofuels: Influence of Strain Selection and Culture Conditions

Vladimir Heredia *[ID], Olivier Gonçalves [ID], Luc Marchal [ID] and Jeremy Pruvost [ID]

GEPEA UMR 6144, Nantes University, F-44600 Saint-Nazaire, France; olivier.goncalves@univ-nantes.fr (O.G.); luc.marchal@univ-nantes.fr (L.M.); jeremy.pruvost@univ-nantes.fr (J.P.)
* Correspondence: rimidalv.marquez@gmail.com

Abstract: Energy-storage metabolites such as neutral lipids and carbohydrates are valuable compounds for liquid biofuel production. The aim of this work is to elucidate the main biological responses of two algae species known for their effective energy-rich compound accumulation in nitrogen limitation and day–night cycles: *Nannochloropsis gaditana*, a seawater species, and *Parachlorella kessleri*, a freshwater species. Lipid and carbohydrate production are investigated, as well as cell resistance to mechanical disruption for energy-rich compound release. Nitrogen-depleted *N. gaditana* showed only a low consumption of energy-storage molecules with a non-significant preference for neutral lipids (TAG) and carbohydrates in day–night cycles. However, it did accumulate significantly fewer carbohydrates than *P. kessleri*. Following this, the highest levels of productivity for *N. gaditana* in chemostat cultures at four levels of nitrogen limitation were found to be 3.4 and 2.2×10^{-3} kg/m^2·d for carbohydrates and TAG, respectively, at $56\%_{NO_3}$ limitation. The cell disruption rate of *N. gaditana* decreased along with nitrogen limitation, from 75% (at $200\%_{NO_3}$) to 17% (at $13\%_{NO_3}$). In the context of potentially recoverable energy for biofuels, *P. kessleri* showed good potential for biodiesel and high potential for bioethanol; by contrast, *N. gaditana* was found to be more efficient for biodiesel production only.

Keywords: renewable energies; biomass; biofuels; microalgae; energy content; bioethanol; biodiesel

1. Introduction

At present, biofuels from microalgae are considered to form part of the solution to replacing fossil fuels and reducing the effects of climate change [1–4]. Biofuels from microalgae can be retrieved in the form of biogas, biodiesel, bioethanol, biobutanol, biomethanol, biohydrogen and others [5–8]. Biodiesel and bioethanol are two of the most promising liquid biofuels derived from microalgae at present [9–12]. Carbohydrates (fermentable sugars) and total fatty acids (TFA) are needed to produce bioethanol and biodiesel. Fatty acids are mainly composed of triacylglycerol (TAG) molecules, which can be accumulated in microalgal cells under conditions of stress [13–16].

As well as the process by which bottlenecks are associated with biomass harvesting and TAG/carbohydrate recovery [17–19], there are several other challenges to overcome in order for these energy-rich metabolites to be produced efficiently, especially when they are produced in variable outdoor conditions.

These include the preferred ways by which microalgae store energy in the molecules concerned [15,20], their resilience to environmental changes [21] and their specific response to light and day–night cycles (DNc) [14,22]. Nonetheless, microalgae biodiversity offers many species capable of adapting to these outdoor conditions with different sets of metabolite profiles [23–29].

Taleb et al. [30] screened 14 microalgae strains for TAG productivity for the purpose of biodiesel production. The most efficient strains found for biodiesel production were *Nannochloropsis gaditana* CCMP527 and *Parachlorella kessleri* UTEX2229, which accumulated up to $56\%_X$ and $40\%_X$ TAG content, respectively. The corresponding maximum areal TAG

productivity was 2.3 and 2.7 $\times$ 10^{-3} kg/m^2·d for *N. gaditana* CCMP527 and *P. kessleri* UTEX2229, respectively, both at the photon flux density (PFD) of 150 μmol/m^2·s.

P. kessleri has been studied previously due to its ability to grow in harsh conditions [31] and produce large amounts of lipids and starch under regular [32,33] and stress conditions [34,35]. Similarly, Taleb et al. [36] reported that the main physiological changes that take place with *P. kessleri* under day–night cycles are linked to the consumption of energy-storage molecules and cell growth. Another detailed study was carried out by Kandilian et al. [35] on the response of *P. kessleri* to different levels of nitrogen limitation and its performance under a continuous light supply; concentrations of nitrate above 3.65 mM were found to trigger stronger carbohydrate accumulation, and low concentrations were found to trigger higher TAG content.

Similarly, *N. gaditana* has been studied for its lipid and carbohydrate production under conditions of stress. Some authors have reported TAG content of up to 40%$_X$ in batch nitrogen-depleted cultures at different light intensities, which highlights the importance of both nitrogen depletion and light for TAG accumulation [37,38]. Additionally, *N. gaditana* was found to produce TAG molecules by the translocation of membrane lipids, *de novo* synthesis, and even recycling other energy-storage molecules [38,39]. Equally important, *N. gaditana* cells exhibited a non-constant mechanical resistance in nitrogen-depleted conditions, which might be linked to changes in the thickness or composition of the cell wall [40–43]. Cell resistance is important, since some processes used in the production of microalgae-based biofuels (e.g., the extraction process on wet biomass) rely on disruption of the cells. The greater the cell resistance, the more energy is needed for cell disruption, thereby impairing the overall energy balance in the biofuel production process. Likewise, the effect of day–night cycles (DNc) on the depletion of energy-storage metabolites is also relevant, as it affects the amount of biofuel that can be produced outdoors. Studies on the physiological response of *N. gaditana* to DNc report gains of about 35% in TAG and 50% in carbohydrates in daytime periods, whereas losses are preferential for TAG in night-time periods due to respiration activity [42].

In summary, the two species of microalgae, *P. kessleri* and *N. gaditana*, are promising for biofuel production. Data are already available in the literature on *P. kessleri* at different nitrogen limitation levels, whereas there are fewer data on *N. gaditana*. This work will evaluate the response of *N. gaditana* to various levels of nitrogen depletion and the potential of both strains as sources for biofuel production, by considering their response in terms of both TAG and carbohydrate production. Cell resistance to mechanical disruption, another relevant parameter for wet-biomass downstream processing, will be also analyzed. These results will be compared with those obtained for *P. kessleri*. Finally, the potentially recoverable energy for liquid biofuels (biodiesel and bioethanol) will be discussed for both strains.

2. Methods

2.1. Strains

The marine microalgae *Nannochloropsis gaditana* was first described by Lubian [44] as part of the *Eustigmatophyceae* class. It has been reported as reproducing asexually by fission. It can reach 3.5–4 $\times$ 2.5–3 μm in size, describing an ellipsoidal shape. *N. gaditana* CCMP527 (National Center for Marine Algae and Microbiota , USA) was the strain used for the experiments in this work.

Parachlorella kessleri is a fresh water microalgae belonging to the *Chlorophyceae* class, with a spherical or ellipsoidal shape. This species has also been reported as reproducing asexually by auto-spores (2, 4, 6 or 8) of around of 2.5–3.5 $\times$ 3–4.5 μm. In the mature stage, it can reach 5–10 μm in size [31,33,45]. In this work, the experiments on *P. kessleri* UTEX2229 (Culture Collection of Algae, University of Texas, USA) by Taleb et al. [30] and Kandilian et al. [35] have been used for comparison with *N. gaditana*.

2.2. Culture Medium

Bold Basal Medium (8.02 mM) was used for the cultivation of *P. kessleri* (the composition of the medium can be found in Kandilian et al. [35]). Artificial Sea Water (ASW) enriched with CONWAY solution, as in Berges et al. [46], was used for the cultivation of *N. gaditana* in this work. The final composition was (mM): NaCl, 248; Na_2SO_4, 17.1; KCl, 5.49; H_3BO_3, 0.259; NaF, 0.045; $MgCl_2$-$6H_2O$, 32.24; $CaCl_2$-$2H_2O$, 0.626; KBr, 0.497; $SrCl_2$-$6H_2O$, 0.056; and $NaHCO_3$, 1.42.

For this work, four levels of nitrogen (N) limitation and one full depletion were used to trigger lipid accumulation. These levels were established as a percentage of the original $NaNO_3$ in the CONWAY formulation ($100\%_{NO_3}$ for 10.6 mM). The limitation levels were 200%, 56%, 46%, 29% and $13\%_{NO_3}$ (21.2, 5.94, 4.88, 3.07 and 1.38 mM, respectively) and $0\%_{NO_3}$ (0 mM) for nitrogen depletion. These values were chosen for the purposes of comparison with the work of Taleb et al. [30] and Kandilian et al. [35] on *P. kessleri*. The $200\%_{NO_3}$ value was used to set the non-limited (replete) physiological state.

2.3. Culture Systems

Two culture systems were used in this study.

The nitrogen-depleted culture was in a 170 L flat-panel airlift photobioreactor (HECtor technology). A detailed description of the photobioreactor (PBR) can be found in Pruvost et al. [47]. This system was operated in batch mode and supplied with artificial LED light to simulate day–night (DNc) cycles, in relation to the average annual irradiation (photon flux density, PFD 270 $\mu mol/m^2 \cdot s$) of Saint-Nazaire, France. Meteorological information on the region was obtained from the Meteonorm database, Switzerland. For the inoculation, a continuous culture of *N. gaditana* in non-limited conditions was established prior to initiating the batch. Once the culture was found to be in an exponential growth phase, enough biomass was harvested to inoculate the batch culture at 0.2 kg/m^3 in a fresh nitrogen-depleted ($0\%_{NO_3}$) medium. The temperature of the culture was regulated at 23 °C and the pH was set at 8 by automatic 98% CO_2 (gas) injection.

For the nitrogen limitation studies, a 1 L flat panel airlift PBR was used. This PBR has been described by Pruvost et al. [20]. The system was operated in continuous mode (chemostat) and under continuous artificial LED light, supplied at 250 $\mu mol/m^2 \cdot s$. The nitrogen-full ($200\%_{NO_3}$) and nitrogen-limited (56%, 46%, 29% and $13\%_{NO_3}$) culture media were supplied continuously using a peristaltic pump (Reglo ICC, Ismatec, Wertheim, Germany) to maintain the dilution rate at 0.01 h^{-1}. The volume in the PBR was maintained and continuously harvested with an overflow into a sterile harvest bottle. The bottle was replaced every time a sample was taken from it. As with the batch experiment, the same non-limited continuous culture was also used to provide the biomass for inoculating the corresponding nitrogen-limited experiments. The temperature was convectively controlled by the room temperature at 23 °C and the pH was set at 8 with the automatic injection of 98% CO_2 (gas).

For each nitrogen limitation level, a steady state was identified in the culture when the daily measurements of biomass, carbohydrate, pigment and total fatty acid concentrations showed no more than 5% variation with respect to the previous day for five consecutive days. Once the steady state was obtained in the culture, cell counting commenced and nitrate concentration was measured. Another level of nitrogen-limited medium was then supplied. The reported measurements at each steady state represent the average over 5 days at steady state. All the previous sampling set-ups were repeated successively using the corresponding medium for each limitation level, from 200% to $13\%_{NO_3}$.

2.4. Cell Disruption Rate and Cell Counting

Cell counting was done by analyzing (in triplicate) a 10 μL aliquot from the nitrogen-limited cultures at steady state. A malassez chamber and an optical microscope equipped with camera (Axio MRC Cam at Axio Scope A1 microscope, Carl Zeiss, Oberkochen, Germany) were used to take 40 pictures of each sample, as described by Zinkoné et al. [48].

Then, using an image treatment software (ImageJ v.1.52o, NIH, Bethesda, MD, USA) and a self-developed algorithm in MATLAB (MathWorks, Natick, Massachusetts, USA), the corresponding image data were processed to obtain statistical information on the number and size of the cells.

To determinate the cell disruption rate, another sample was adjusted to obtain 30 mL at a biomass concentration of 1 kg/m^3 using a phosphate buffer saline (PBS) solution. This was done to standardize the measurements from different nitrogen limitations and avoid the effect of concentration in the disruption system. The preparation was then passed through a high-pressure homogenization device (TS5, Constant Systems Limited, Daventry, UK) at 1750 bar.

The cell disruption rate (τ_D), which represents the mechanical resistance of cells, is reported below as the complementary proportion of the ratio of cells counted after bead milling, compared to those counted before the process.

2.5. Dry Weight Measurement

For biomass concentration analysis, 10 mL samples were collected in triplicate and passed through a pre-weighed 0.45 µm glass-fiber filter (Whatman GF/F, Cytiva, Marlborough, Massachusetts, USA). The filters were then washed with 1.19 M NH_4HCO_2 and MiliQ water to remove residue salts from the culture medium. The filters were left at 103 °C for about 1 h or until the weight was stable. Biomass concentration *X* is reported as the difference in weight before filtration and after, in terms of the volume used. Similarly, pigment, carbohydrate, TFA and TAG content are reported as a percentage of the biomass ($\%_X$). Biomass concentration was used to determine volumetric productivity P_X and areal productivity S_X. The corresponding definitions can be found in Pruvost et al. [49].

2.6. Pigment Content

Pigment content analysis was carried out in accordance with Ritchie [50] and Strickland and Parsons [51]. Samples of 0.5 mL were centrifuged at 6000 RFC, 4 °C for 10 min. The pellet was resuspended in 1.5 mL of methanol anhydrous 99.8%. After 1 min in a sonic bath, samples were incubated at 45 °C for 50 min. Then, the supernatant was recovered after centrifugation, and light absorption at 750, 665, 652 and 480 nm was measured (V-730, Jasco, Easton, MD, USA). The pigment concentrations were obtained using the equations from the literature previously cited. Pigment content is expressed as a percentage of the overall dry biomass ($\%_X$ Pig).

Additionally, the ratio 480/662 nm (stress index) was calculated as a representation of the carbon/nitrogen content and level of stress in the cell. The higher the value, the greater the carotenoid content compared to chlorophyll. This indicates that nitrogen limitation has a direct effect, triggering the decrease in chlorophyll compared to carotenoids [52].

2.7. Total Fatty Acid and Triacylglycerol Content

The whole-cell extraction method described by Van Vooren et al. [53] was applied to quantify the total fatty acid (TFA) and triacylglycerol (TAG). Following the protocol, a 30 mL sample was centrifuged for 10 min at 6000 RFC and 4 °C. The pellet was recovered and freeze-dried for 24 h. A total of 6 mL of chloroform/methanol 2:1 *v/v* (Fisher Sci, Hampton, New Hampshire, USA) and 0.01% *w/w* of butylated hydroxytoluene was then added to the samples immediately and left for 6 h in incubation at 25 °C. Following sample sedimentation, the solvent was recovered and analyzed for TFA concentration by gas chromatography with a flame ionization detector, GC–FID (Thermo Fisher Sci, Waltham, Massachusetts, USA), and for TAG concentration by high-performance thin-layer chromatography, HPTLC (CAMAG, Muttenz, Switzerland). TFA/TAG content is expressed as a percentage of the overall dry biomass ($\%_X$ TFA/TAG).

After determining the TAG content, the corresponding volumetric and areal productivities (P_{TAG}, S_{TAG}) were also determined, in accordance with Pruvost et al. [49].

2.8. Total Carbohydrate Content

Total carbohydrates were measured following the protocol developed by DuBois et al. [54]. A 10 mL sample was centrifuged for 10 min at 6000 RFC and 4 °C. The pellet was recovered and resuspended in 1 mL of MiliQ water. A 0.5 mL aliquot was mixed with 0.5 mL of phenol solution (0.53 M) and three consecutive 2.5 mL doses of 97% H_2SO_4. Between each dose, the solution was vigorously agitated. The reaction was then left for 30 min at room temperature and wet-bath-incubated at 35 °C for 30 min, after which absorbance was measured at 483 nm (V-730, Jasco, Easton, MD, USA). A calibration curve from 0.025 to 0.1 g/L of glucose was prepared to calibrate the method and subsequently obtain the total carbohydrate concentration of the sample. The total carbohydrate content is expressed as a percentage of the overall dry biomass ($\%_X$ Sg).

The areal productivity was also calculated based on carbohydrate content (S_{Sg}), using the same method as for TAG values.

2.9. Nitrate Concentration Measurement

Once a steady state was reached in the continuous cultures, the outflow culture medium was recovered for nitrate measurement. A volume of 3–5 mL was filtered using a 0.2 μm acetate cellulose filter (Minisart, Sartorius, Gottingen, Germany). The sample was injected into an ion chromatography system (ICS 900, Thermo Fisher Sci, Waltham, Massachusetts, USA) to find the NO_3^- ion concentration. If needed, concentration was adjusted by dilution with MiliQ water to make it readable under the ion chromatography method. Using the NO_3^- concentration, the Nitrogen uptake yield ($Y_{N/X}$)was calculated with the equation

$$Y_{N/X} = \Delta N_t / X \tag{1}$$

where ΔN_t is the difference between the NO_3^- concentration in the supplied and worn-out culture media.

2.10. Potentially Recoverable Energy Calculation

A theoretical estimate of the amount of energy that can be recovered from microalgae was calculated as the sum of the energy derived from the biofuels potentially obtained from the TAG (converted into biodiesel) and carbohydrates (converted into bioethanol) produced. This was expressed per unit of time and illuminated surface for simplicity of comparison with other applications.

First, the energy from biodiesel via TAG transesterification (E_{BioD} in J/m²·d) was obtained

$$E_{BioD} = (S_{TAG} / MW_{algallipids}) \cdot \eta_{E,TAG} \cdot 3 \cdot Y_{Trans} \cdot MW_{FAME} \cdot \Delta H^{\circ}_{comb,BioD} \tag{2}$$

where $MW_{algallipids}$ is the molecular weight of the lipids (and TAG molecules) from the harvested biomass, MW_{FAME} is the molecular weight of fatty acid methyl esters (FAME, biodiesel) (g/mol), $\eta_{E,TAG}$ is the efficiency of TAG recovery, Y_{Trans} is the efficiency of the transesterification stage, and $\Delta H^{\circ}_{comb,BioD}$ is the heat of combustion of biodiesel (26.7 MJ/kg_{BioD}). The value of 3 is the stoichiometric coefficient of the FAME product in the transesterification step.

To analyze the biodiesel production, it was proposed that about 80% of the TAG produced was actually recovered. This value may be accomplished using the wet-extraction process [55,56]. Transesterification was then proposed based on a conversion yield of 98%. Note, however, that such values require six moles of alcohol per mole of triglyceride [57]. For the molecular weight of the fatty acid methyl esters (FAME, biodiesel), the calculation was based on the proposed fatty acid profile of *Botryococcus braunii*, given in Ashokkumar et al. [58]. The corresponding heat of combustion of biodiesel is derived from this value.

Second, the energy from bioethanol via carbohydrate fermentation (E_{BioE} in J/m$^2\cdot$d) is the product of

$$E_{BioE} = S_{Sg} \cdot \eta_{E,Sg} \cdot Y_{Fer} \cdot \Delta H^\circ_{comb,BioE} \tag{3}$$

where $\eta_{E,Sg}$ is the efficiency of fermentable carbohydrate recovery, Y_{Fer} is the bioethanol conversion yield at the fermentation step and $\Delta H^\circ_{comb,BioE}$ is the heat of combustion of bioethanol (40.4 MJ/kg$_{BioE}$).

The term $\eta_{E,Sg}$ represents the recovery and acid hydrolysis of the total carbohydrate, according to Karemore and Sen [9]. The fermentation yield from the same work was 0.23 g of bioethanol per gram of fermentable sugar. Bioethanol was produced by converting 90% of the fermentable sugars. The value was reported to be 40% of the theoretical value for the *Saccharomyces cerevisiae* fermentation.

Finally, the total value of the recoverable fuel energy (J/m$^2\cdot$d) was estimated as

$$E_P = E_{BioD} + E_{BioE} \tag{4}$$

3. Results and Discussion

3.1. Response of N. gaditana to Nitrogen Depletion in Day–Night Cycles

Investigating the effects of nitrogen depletion on *N. gaditana* cultivated in day–night cycles (DNc) and batch mode was based on the approach described by Taleb et al. [36] for *P. kessleri* in a 1 L PBR. For the present study, a plateau was obtained after 168 h. Since the light source remained unchanged (same DNc's) during the whole cultivation time, the plateau may indicate nitrogen depletion (i.e., no growth). The culture was then maintained for 11 days, as in the above-mentioned reference, to allow lipid accumulation during this time.

The final composition of the culture is shown in Table 1. *N. gaditana* was found to be considerably less productive than *P. kessleri* under the same culture conditions, with biomass concentrations of 0.9 and 1.3 kg/m^3, respectively. The energy-storage molecules in *N. gaditana* attained 43cX: 17%$_X$ carbohydrates and 26%$_X$ TFA. About 70% of the TFA consisted of TAG molecules at this stage (18%$_X$).

Table 1. Biochemical comparison of *P. kessleri* and *N. gaditana* at the end of batch culture under simulated DNc (11 days). Standard error for n = 3.

Strain	X kg/m (SE)	Carbohydrates %$_X$ (SE)	TFA %$_X$ (SE)	TAG %$_X$ (SE)	Reference
P. kessleri	1.3 (0.04)	46 (2)	35	35	Taleb et al. [36]
N. gaditana	0.9 (0.04)	17 (1)	26 (0.2)	18	Present study

It is interesting to compare the difference in the accumulation preference between energy-storage molecules. Carbohydrate concentration was 0.65 times less than that of TFA in *N. gaditana*, whereas the carbohydrates in *P. kessleri* were about 1.3 times more than the concentration of TFA. This difference could be explained by the preference of *P. kessleri* to accumulate carbohydrates as an energy-storage molecule, to tolerate the dark periods during DNc. *P. kessleri* was indeed reported to consume up to 10 and 5%$_X$ of carbohydrates and TAG storage, respectively, in DNc (reported as non-significant) [36]. In the present work *N. gaditana* was found to consume only 1.4 and 1%$_X$ of carbohydrates and TAG, respectively, for the dark periods between 137 and 167 h (Figure 1). This could also explain the difference in biomass development between the two strains in DNc. Therefore, the fact that the energy-rich compounds of *N. gaditana* do not vary greatly during the night could be beneficial for biofuel production, because the productivity would not be greatly affected by outdoor cultivation in actual day–night cycles. More detailed studies will be required, since other parameters, such as temperature and night duration, could also influence the consumption dynamics of energy-rich compounds.
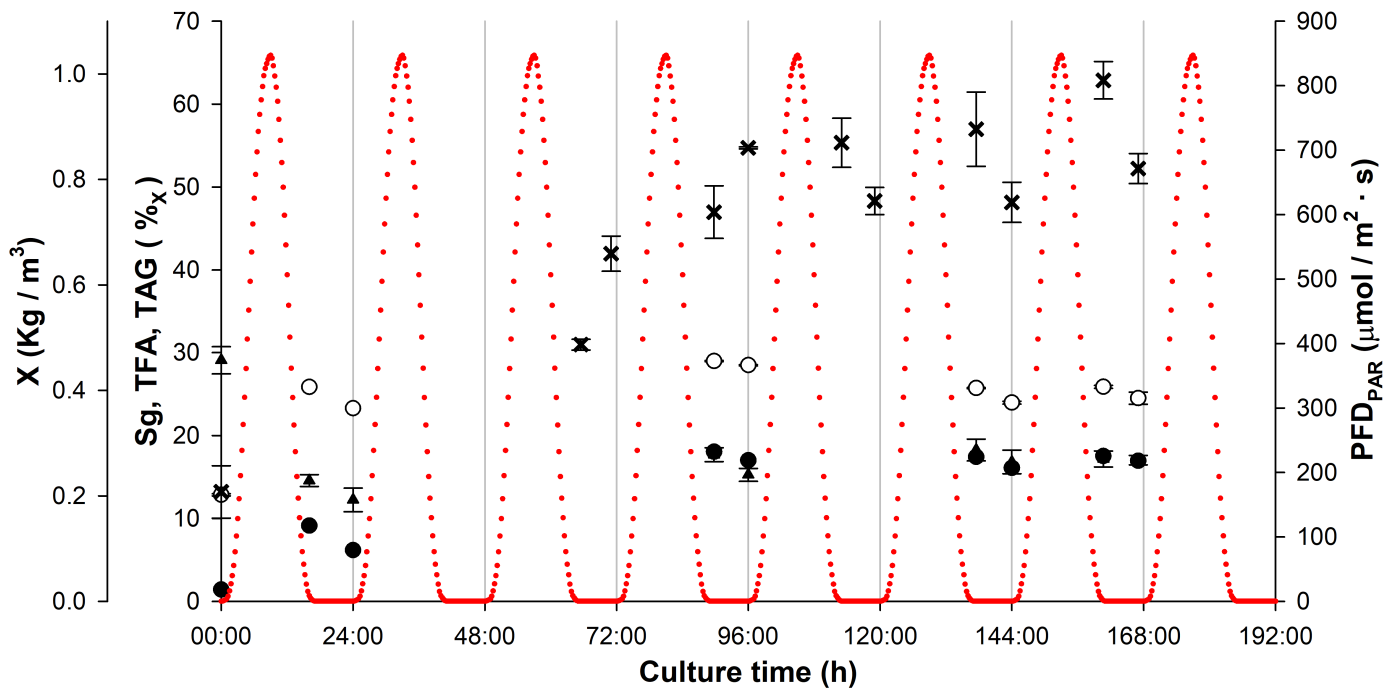
Figure 1. Physiological changes in *N. gaditana* under day–night cycles in depleted conditions. Triangles represent total carbohydrates; white circles represent total fatty acids; black circles represent tricylglycerol (TAG); red dots represent the photon flux density supplied to the PBR.

The areal TAG productivity under DNc obtained in the present work was compared with the results obtained by Taleb et al. [36] for both *N. gaditana* and *P. kessleri*, under continuous light and DNc regimes. In the present work, *N. gaditana* achieved 1.3×10^{-3} kg/m^2·d in TAG at the end of 7 days under batch nitrogen depletion in simulated DNc. This value is around 30% less than the final areal productivity reported for *P. kessleri* in the same culture conditions (DNc). It can also be observed that the difference between strains is only 15% under continuous light, which could also be related to the night consumption of energy-storage molecules.

Figure 2 shows a complementary study of the mechanical resistance of the cells. In batch-cultivated, nitrogen-depleted medium and continuous light (culture data not shown) *N. gaditana* shows a more marked difference in the cell disruption rate compared to nitrogen-replete conditions. In nitrogen-depleted conditions, cell disruption was 11% (SE 5%), which is 85% less than the disruption rate found in replete conditions [30]. This trend, which indicates an increase in the mechanical resistance of the cells in nitrogen-depleted conditions, has also been observed by Angles et al. [55].
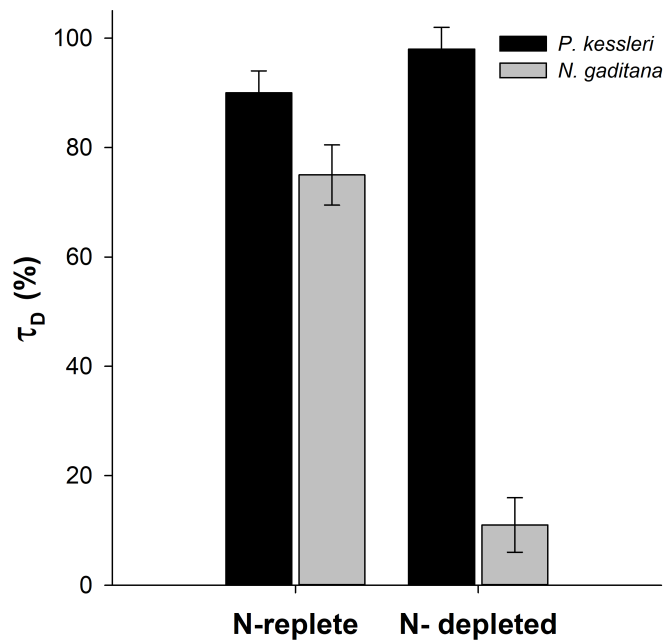
Figure 2. Comparison of cell disruption (at 1750 bar) for *N. gaditana* and *P. kessleri* [30] in two physiological states.

3.2. N. gaditana Culture under Nitrogen Limitation and Continuous Mode

Nitrogen limitation applied to continuous culture proved useful in obtaining a biomass rich in the relevant storage molecules, in a single production step [22,59]. The response of *N. gaditana* to four consecutive levels of nitrogen limitation in continuous mode (56%, 46%, 29% and 13%$_{NO_3}$) was investigated. The results were compared to those obtained for *P. kessleri* under the same conditions as used by Kandilian et al. [35]. The PBR was operated in continuous mode until steady-state was achieved, to allow the microalgae to adapt to each NO_3^- concentration (around 20 days between each steady state). Continuous light (photon flux density 250 µmol/m^2·s) and CO_2 supply were regulated so as not to limit cell growth. The results are given in Table 2; Figure 3 shows the main results.

Table 2. Physiological changes of *N. gaditana* at steady state for several levels of nitrogen limitation. SE for standard error with n = 4.

| Limitation %$_{NO_3}$	X kg/m^3 (SE)	Pigments %$_X$ (SE)	TFA %$_X$ (SE)	TAG %$_X$ (SE)	Carbohydrates %$_X$ (SE)	τ_D %$_X$ (SE)	$Y_{NO_3^-/X}$ mg$_{NO_3^-}$/g$_X$	Stress Index
200	2.13 (0.04)	2.54 (0.12)	11.11 (0.60)	1.78 (0.10)	19.01 (1.77)	75.00 (11.00)	411.4	0.55
56	2.06 (0.02)	1.35 (0.04)	25.22 (0.72)	14.78 (1.08)	22.98 (0.88)	73.00 (2.07)	188.7	0.72
46	1.80 (0.03)	0.97 (0.04)	24.23 (1.00)	14.42 (1.01)	17.59 (0.58)	63.00 (3.43)	201.3	0.95
29	1.39 (0.02)	0.90 (0.03)	30.87 (1.23)	19.29 (0.37)	16.72 (0.69)	43.32 (3.81)	105.1	1.36
13	0.89 (0.02)	0.64 (0.02)	37.34 (1.72)	24.24 (1.06)	18.48 (1.33)	17.00 (2.91)	98.4	1.70
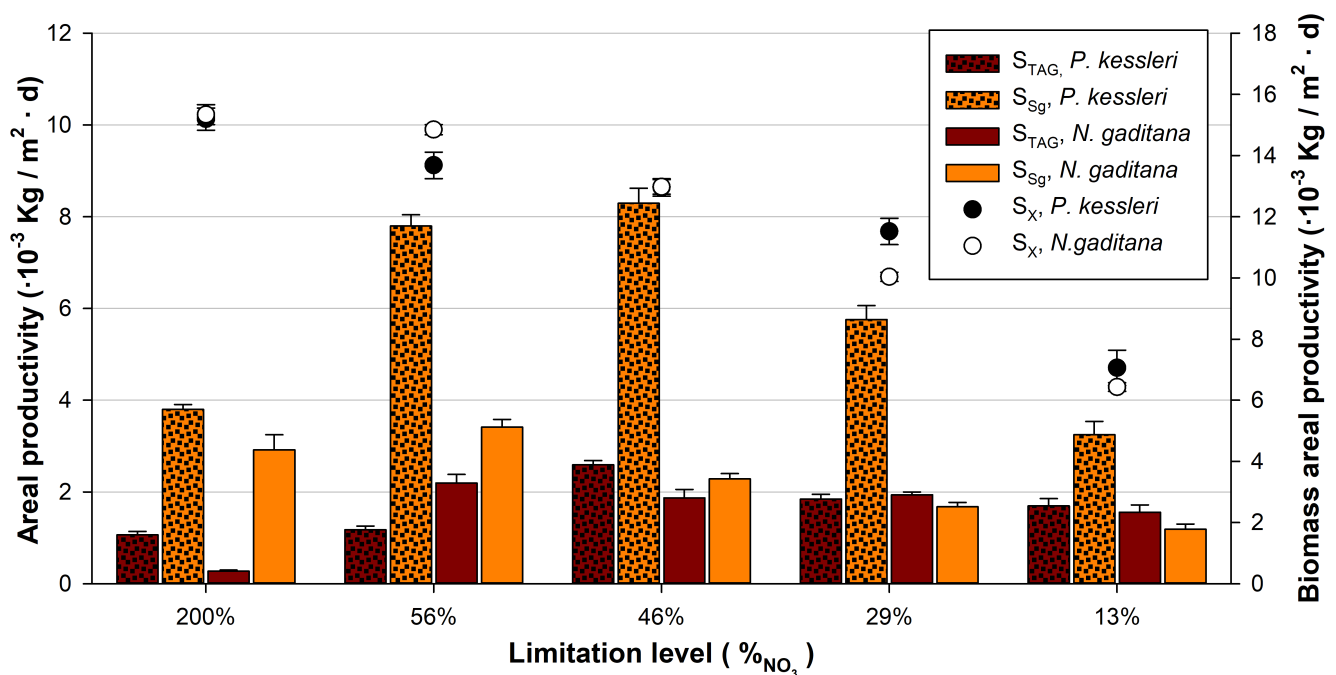
Figure 3. Areal productivities for Biomass (S_X), TAG (S_{TAG}) and carbohydrates (S_{Sg}) of *N. gaditana* and *P. kessleri* at steady state for several levels of nitrogen limitation. Error bars in *N. gaditana* are for SE with n = 4, for the rest, refer to Kandilian et al. [35].

3.2.1. Nitrogen Uptake and Stress Index

The nitrogen uptake yield ($Y_{NO_3^-/X}$) as a value for indicating the ability of the cell to assimilate the surrounding nitrogen sources, and the stress index as an indirect correlation of the C:N ratio [52], were calculated at steady state for each limitation level. Note that all the limited cultures left an undetectable amount of NO_3^- in the medium (<5 mg_{NO_3}/L, below the detection level), except for the $200\%_{NO_3}$ limitation. This corroborates the level of nitrogen depletion expected to stress the cultures by limiting the nitrogen source.

The non-limited culture was characterized for the highest nitrogen uptake yield, 411 g_{NO_3}/g_X. The value was reduced to 189 and 201 g_{NO_3}/g_X for the two subsequent limitation values, 56% and $46\%_{NO_3}$, respectively. Then, values were reduced again by half, for stronger nitrogen limitations: 105 and 98 g_{NO_3}/g_X at 29% and $13\%_{NO_3}$, respectively. Rafay et al. [60] recently calculated the maximum specific nitrate uptake of *N. gaditana* as 210 ± 11.2 mg_{NO_3}/g_X in a batch culture (F/2 medium for initial NO_3^- 100 mg/L), which falls within the range of values obtained in the present study.

As mentioned above, a decrease in pigment content is another physiological change that takes place in nitrogen-limited cultures [22,61]. Stress levels, along with nitrogen limitation, can be monitored by measuring the cell pigment content [52]. Specifically, the stress index behaved in a similar but inverted trend compared to the previously reported nitrogen uptake values. The representative stress index for the non-limited culture was 0.55. For higher limitations, the value increased progressively to 1.70 at $13\%_{NO_3}$. Dortch [62] showed that as soon as external nitrogen starts to limit growth, phytoplankton may accumulate pools of un-assimilated nitrogen, allowing the cell to rapidly react to changes in medium composition (which may be read as the small stress index or C:N ratio). Thereafter, while the surrounding nitrogen concentration remains low, the cells consume this nitrogen pool first, before any other organic nitrogen stock (proteins or amino acids) and then re-adapt to the new environment. This leads to a reduction in the total nitrogen in the cell, increasing the stress index.

3.2.2. Biomass, TAG and Total Carbohydrates

The total biomass concentration of *N. gaditana* decreased from 2.13 kg/m^3 in non-limited conditions ($200\%_{NO_3}$) to 0.89 kg/m^3 at $13\%_{NO_3}$. The total biomass did not change

at the same rate as the nitrogen limitation. Reducing the nitrogen concentration from 200 to 56%$_{NO_3}$ only reduced the biomass concentration by 3%. However, a higher limitation, from 29 to 13%$_{NO_3}$, reduced the biomass concentration by 36%. The biomass trend is very similar to that noted with *P. kessleri*, as reported by Kandilian et al. [35]. The most notable difference between the two strains is related to the level of stress needed to accumulate energy-storage molecules.

When *N. gaditana* is in favorable growth conditions, a small fraction of the total biomass (2%$_X$ TAG) appears as TAG molecules (which are 16% of TFA). In comparison, as can be noted in Table 2, when limitations were introduced, both strains gained up to 24 %$_X$ TAG at the highest limitation. However, strains showed differences in nitrogen limitation levels: *P. kessleri* needed between 29 and 46 %$_{NO_3}$ limitation to obtain an average 17%$_X$ TAG; *N. gaditana* immediately achieved 15%$_X$ TAG at the first limitation value (56 %$_{NO_3}$). This might be a useful optimization indicator for *N. gaditana*, since low limitation values do not compromise biomass production as much as higher limitations do.

Regarding carbohydrates, *N. gaditana* does not accumulate as much as *P. kessleri* (Table 2). In optimal growth conditions, it accumulates 19%$_X$ in carbohydrates, which, at this point, is higher than the TAG content. A limitation of 56%$_X$ therefore triggers maximum carbohydrate content up to 23%$_X$. At the lowest limitation, only 18%$_X$ carbohydrates are accumulated, and at this point there are already more TAG molecules accumulated in the cell. On the other hand, the values reported for *P. kessleri* indicate that no less than 45%$_X$ carbohydrates are achieved for all limitations (maximum 64%$_X$ carbohydrates at 46%$_{NO_3}$). It therefore seems that *P. kessleri* has a marked storage preference for carbohydrates over TAG molecules in all the nitrogen-limited conditions tested here. However, although *N. gaditana* has a slight preference for carbohydrates at medium limitations (56% and 46%$_{NO_3}$) and more for TAG at stronger limitations (29% and 13%$_{NO_3}$), the difference is balanced between the two energy-storage molecules compared to *P. kessleri*. Simionato et al. [38] mention the possibility of some sugars being recycled into TAG molecules, which may explain the low carbohydrate content of *N. gaditana*.

Figure 3 shows the areal productivity for biomass, TAG and carbohydrates. The combined effect of the growth and composition of biomass in *N. gaditana* revealed the maximum levels of carbohydrate and TAG productivity to be equal to 3.41 and 2.19 $\times$ 10^{-3} kg/m^2·d (SE 0.17 and 0.19), respectively, at 56%$_{NO_3}$ limitation.

Carbohydrate productivity for *N. gaditana* did not vary widely within the 56%$_{NO_3}$ limitation compared to the non-limited experiment (200%$_{NO_3}$). However, it varied significantly at lower limitation levels, passing from 2.28 $\times$ 10^{-3} kg/m^2·d at 46%$_{NO_3}$ to 1.19 $\times$ 10^{-3} kg/m^2·d at 13%$_{NO_3}$ (SE 0.12 and 0.11, respectively). Similarly, TAG productivity remained almost unvaried for limitations at 56%, 46% and 29%$_{NO_3}$, achieving values of 2.19, 1.87 and 1.94 $\times$ 10^{-3} kg/m^2·d (SE 0.19, 0.18, 0.07), respectively. Although the limitation level of 13%$_{NO_3}$ triggered the highest content (24.2%$_X$), TAG productivity reached only 1.56 $\times$ 10^{-3} kg/m^2·d (SE 0.16) at the lowest biomass productivity rate.

In comparison, *P. kessleri* [35] produced the largest amount of carbohydrates (S$_{Sg}$) for limitation levels between 56%$_{NO_3}$ and 29%$_{NO_3}$ (the highest at 8.3 $\times$ 10^{-3} kg/m^2·d, at a 46%$_{NO_3}$ limitation). The maximum TAG productivity for *P. kessleri* was also observed at 46%$_{NO_3}$ limitation (2.6 $\times$ 10^{-3} kg/m^2·d).

It is also interesting to note that, in large-scale outdoor production, it would be harder to apply the given limitation levels precisely. It is nonetheless important to know the limitation levels that trigger the greatest TAG and carbohydrate productivity

3.2.3. Cell Resistance

The fact that *N. gaditana* is more resistant to mechanical stress in nitrogen-depleted conditions has been reported previously in the literature [40,43,55] and is confirmed in the present batch experiment. A more detailed evolution of this change at different levels of nitrogen limitation is given in Table 2.

A non-limited culture of *N. gaditana* can be disrupted at 75% in a single stage through high-pressure homogenization at 1750 bar. This resistance is maintained with a low limitation of $56\%_{NO_3}$, but the disruption rate τ_D was reduced to 63% at $46\%_{NO_3}$ limitation, and fell to 17% at the lowest limitation. Cell concentration was rejected as an explanation for this phenomenon since all the samples were prepared at 1 kg/m^3. An evolution in the cell wall composition and thickness could be the explanation for this [39,40,43,63,64].

The cell resistance of microalgae cultivated in nitrogen-depleted conditions has proven to be an important factor for recovering TAG and carbohydrate molecules in wet-biomass treatment. The values shown here imply that even if productivity is high at some limitation levels, not all the compounds can be recovered if the cell is resistant to the disruption (or more energy is required to obtain sufficient cell disruption). In other words, the final metabolite productivity and overall efficiency of the whole process depends on how easy it is to recover these compounds in this physiological state. The results affect the entire energy investment in the biofuel production process.

3.3. Potentially Recoverable Energy

Previous results have shown that the nitrogen limitation levels applied may impact both TAG and carbohydrate productivity in the microalgae cells in different ways. At some levels of limitation, more carbohydrates are produced than TAG, and the reverse is true for others levels of limitation. This could impact the amount of biofuel energy that can be obtained. For this reason, a theoretical analysis of the potentially recoverable energy (E_P) from the two strains shown above, cultivated in nitrogen-limited conditions, is discussed here. This analysis is based on Equation (4), using the values given in Table 3.

Table 3. Values used to calculate recoverable fuel energy of *N. gaditana* and *P. kessleri*.

		Units	**Reference**
$\Delta H^{\circ}_{comb,BioE}$	26.7	MJ/kg	Yüksel and Yüksel [65]
$\Delta H^{\circ}_{comb,BioD}$	40.4	MJ/kg	Ashokkumar et al. [58]
$MW_{algallipids}$	920	g/mol	Ashokkumar et al. [58]
MW_{FAME}	299.32 *	g/mol	Ashokkumar et al. [58]
Y_{Fer}	0.23	$\text{kg}_{BioE}/\text{kg}_{Sg}$ **	Karemore and Sen [9]
Y_{Trans}	98	%	Fukuda et al. [57]
$\eta_{E,TAG}$	80	%	Proposed
$\eta_{E,Sg}$ **	89.6	%	Karemore and Sen [9]

* Based on the fatty acid profile reported; ** Fermentable carbohydrates.

The results in Figure 4 show the impact that the obtained TAG and carbohydrate productivity have on a theoretical biofuel process, in terms of global energy valorization. *Nannochloropsis gaditana* achieved maximum energy values of 67.8 and 18.7 $\text{J/m}^2 \cdot \text{d}$ for biodiesel and bioethanol, respectively, at the $56\%_{NO_3}$ limitation level. The corresponding total amount of recoverable energy E_P was, therefore, 86.6 $\text{J/m}^2 \cdot \text{d}$. Note that the E_P values for *N. gaditana* did not take into account the changing disruption rates presented in Table 2.

In comparison, the maximum amount of potentially recoverable energy E_P from *P. kessleri* [35] was 128 $\text{J/m}^2 \cdot \text{d}$ at the $46\%_{NO_3}$ limitation level, with 47 $\text{J/m}^2 \cdot \text{d}$ accounted for by the energy obtained from bioethanol and 81 $\text{J/m}^2 \cdot$ by biodiesel. Note that although the carbohydrate productivity of *P. kessleri* at $56\%_{NO_3}$ was almost twice that of *N. gaditana* at the same limitation level, the total amount of recoverable energy from *N. gaditana* at the same level was higher due to the greater proportion of biodiesel energy (heat of combustion 40.4 MJ/kg) and also the greater TAG content.
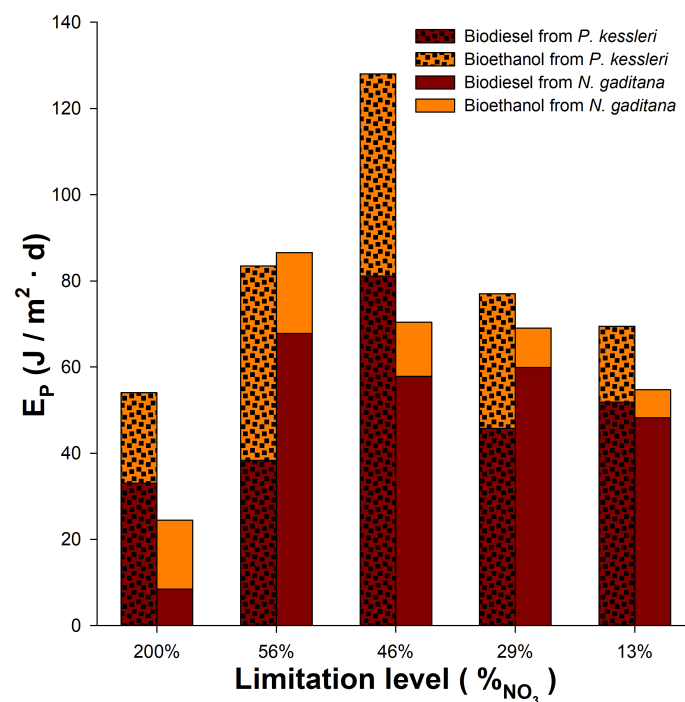
Figure 4. Potentially recoverable energy values for *N. gaditana* and *P. kessleri* obtained in continuous nitrogen-limited culture.

In summary, carbohydrate productivity with *Nannochloropsis gaditana* is not as great as with *Parachlorella kessleri*. The latter has more potential for dual-biofuel valorization (biodiesel and bioethanol), where more energy can be obtained from the same amount of biomass produced due to the large accumulation of both carbohydrates and TAG. However, *N. gaditana* may be of interest in terms of biodiesel production in particular, due to its preference for TAG accumulation.

4. Conclusions

This study has demonstrated the effect that nitrogen limitation has on the physiology of *Nannochloropsis gaditana*. During day–night cycles, *N. gaditana* did not show any preference or significant TAG or carbohydrate consumption during the night period. This stability could be beneficial in outdoor cultivation. Under continuous light and nitrogen-limited conditions, the highest carbohydrate and TAG productivity of *N. gaditana* was 3.41 and 2.19×10^{-3} kg/m^2·d, respectively, for the 56%$_{NO_3}$ limitation in continuous mode (PFD 250 µmol/m^2·s). The disruption rate τ_D of *N. gaditana* decreased significantly by around 77% from non-limited conditions to the lowest limitation level. This trend may compromise the eventual recovery of metabolites. The same analysis was applied to data available in the literature for *Parachlorella kessleri*. The results showed that under moderate limitation levels, *P. kessleri* produces larger amounts of energy-storage molecules, which should be easier to recover due to the high cell disruption rate. This, in addition to a high rate of carbohydrate production, is encouraging for the development of both biodiesel and bioethanol. However, *N. gaditana* remains a promising producer of energy-storage metabolites for biodiesel production, using seawater in particular.

Author Contributions: conceptualization, V.H.; methodology, V.H. and J.P.; validation, J.P.; formal analysis, V.H.; investigation, V.H. and J.P.; writing—original draft preparation, V.H. and J.P.; writing—review and editing, V.H., O.G., L.M. and J.P.; visualization, V.H. and J.P.; supervision, O.G., L.M. and J.P.; project administration, V.H. and J.P. All authors have read and agreed to the published version of the manuscript.

References

1. Ponton, J.W. Biofuels: Thermodynamic sense and nonsense. *J. Clean. Prod.* **2009**, *17*, 896–899. [CrossRef]
2. Brennan, L.; Owende, P. Biofuels from microalgae—A review of technologies for production, processing, and extractions of biofuels and co-products. *Renew. Sustain. Energy Rev.* **2010**, *14*, 557–577. [CrossRef]
3. Fortman, J.L.; Chhabra, S.; Mukhopadhyay, A.; Chou, H.; Lee, T.S.; Steen, E.; Keasling, J.D. Biofuel alternatives to ethanol: Pumping the microbial well. *Trends Biotechnol.* **2008**, *26*, 375–381. [CrossRef] [PubMed]
4. Timilsina, G.R.; Shrestha, A. How much hope should we have for biofuels? *Energy* **2011**, *36*, 2055–2069. [CrossRef]
5. Dębowski, M.; Zieliński, M.; Kazimierowicz, J.; Kujawska, N.; Talbierz, S. Microalgae cultivation technologies as an opportunity for bioenergetic system development—Advantages and limitations. *Sustainability* **2020**, *12*, 9980. [CrossRef]
6. Shuba, E.S.; Kifle, D. Microalgae to biofuels: 'Promising' alternative and renewable energy, review. *Renew. Sustain. Energy Rev.* **2018**, *81*, 743–755. [CrossRef]
7. Ganesan, R.; Manigandan, S.; Samuel, M.S.; Shanmuganathan, R.; Brindhadevi, K.; Lan Chi, N.T.; Duc, P.A.; Pugazhendhi, A. A review on prospective production of biofuel from microalgae. *Biotechnol. Rep.* **2020**, *27*, e00509. [CrossRef]
8. Adeniyi, O.M.; Azimov, U.; Burluka, A. Algae biofuel: Current status and future applications. *Renew. Sustain. Energy Rev.* **2018**, *90*, 316–335. [CrossRef]
9. Karemore, A.; Sen, R. Downstream processing of microalgal feedstock for lipid and carbohydrate in a biorefinery concept: A holistic approach for biofuel applications†. *RSC Adv.* **2016**, *6*, 29486–29496. [CrossRef]
10. Williams, P.J.B.; Laurens, L.M. Microalgae as biodiesel & biomass feedstocks: Review & analysis of the biochemistry, energetics & economics. *Energy Environ. Sci.* **2010**, *3*, 554–590. [CrossRef]
11. Zhu, L.; Nugroho, Y.K.; Shakeel, S.R.; Li, Z.; Martinkauppi, B.; Hiltunen, E. Using microalgae to produce liquid transportation biodiesel: What is next? *Renew. Sustain. Energy Rev.* **2017**, *78*, 391–400. [CrossRef]
12. De Farias Silva, C.E.; Bertucco, A. Bioethanol from microalgae and cyanobacteria: A review and technological outlook. *Process. Biochem.* **2016**, *51*, 1833–1842. [CrossRef]
13. Breuer, G.; Lamers, P.P.; Martens, D.E.; Draaisma, R.B.; Wijffels, R.H. Effect of light intensity, pH, and temperature on triacylglycerol (TAG) accumulation induced by nitrogen starvation in Scenedesmus obliquus. *Bioresour. Technol.* **2013**, *143*, 1–9. [CrossRef]
14. Bonnefond, H.; Moelants, N.; Talec, A.; Bernard, O.; Sciandra, A. Concomitant effects of light and temperature diel variations on the growth rate and lipid production of Dunaliella salina. *Algal Res.* **2016**, *14*, 72–78. [CrossRef]
15. Vitova, M.; Bisova, K.; Kawano, S.; Zachleder, V. Accumulation of energy reserves in algae: From cell cycles to biotechnological applications. *Biotechnol. Adv.* **2014**, *33*, 1204–1218. [CrossRef]
16. Naik, S.N.; Goud, V.V.; Rout, P.K.; Dalai, A.K. Production of first and second generation biofuels: A comprehensive review. *Renew. Sustain. Energy Rev.* **2010**, *14*, 578–597. [CrossRef]
17. Scott, S.A.; Davey, M.P.; Dennis, J.S.; Horst, I.; Howe, C.J.; Lea-Smith, D.J.; Smith, A.G. Biodiesel from algae: Challenges and prospects. *Curr. Opin. Biotechnol.* **2010**, *21*, 277–286. [CrossRef]
18. Yuan, J.; Kendall, A.; Zhang, Y. Mass balance and life cycle assessment of biodiesel from microalgae incorporated with nutrient recycling options and technology uncertainties. *GCB Bioenergy* **2015**, *7*, 1245–1259. [CrossRef]
19. Kim, J.; Yoo, G.; Lee, H.; Lim, J.; Kim, K.; Kim, C.W.; Park, M.S.; Yang, J.W. Methods of downstream processing for the production of biodiesel from microalgae. *Biotechnol. Adv.* **2013**, *31*, 862–876. [CrossRef]
20. Pruvost, J.; Van Vooren, G.; Cogne, G.; Legrand, J. Investigation of biomass and lipids production with Neochloris oleoabundans in photobioreactor. *Bioresour. Technol.* **2009**, *100*, 5988–5995. [CrossRef]
21. Caperon, J.; Meyer, J. Nitrogen-limited growth of marine phytoplankton-I. changes in population characteristics with steady-state growth rate. *Deep-Sea Res. Oceanogr. Abstr.* **1972**, *19*, 601–618. [CrossRef]
22. Kandilian, R.; Pruvost, J.; Legrand, J.; Pilon, L. Influence of light absorption rate by Nannochloropsis oculata on triglyceride production during nitrogen starvation. *Bioresour. Technol.* **2014**, *163*, 308–319. [CrossRef] [PubMed]
23. Ho, S.H.; Huang, S.W.; Chen, C.Y.; Hasunuma, T.; Kondo, A.; Chang, J.S. Bioethanol production using carbohydrate-rich microalgae biomass as feedstock. *Bioresour. Technol.* **2013**, *135*, 191–198. [CrossRef] [PubMed]
24. Beer, L.L.; Boyd, E.S.; Peters, J.W.; Posewitz, M.C. Engineering algae for biohydrogen and biofuel production. *Curr. Opin. Biotechnol.* **2009**, *20*, 264–271. [CrossRef]

25. Borowitzka, M.A.; Moheimani, N.R. *Algae for Biofuels and Energy*; Springer: Dordrecht, The Netherlands, 2013; pp. i–xii. [CrossRef]

26. Ma, Y.; Wang, Z.; Yu, C.; Yin, Y.; Zhou, G. Evaluation of the potential of 9 Nannochloropsis strains for biodiesel production. *Bioresour. Technol.* **2014**, *167*, 503–509. [CrossRef] [PubMed]

27. Suganya, T.; Varman, M.; Masjuki, H.H.; Renganathan, S. Macroalgae and microalgae as a potential source for commercial applications along with biofuels production: A biorefinery approach. *Renew. Sustain. Energy Rev.* **2016**, *55*, 909–941. [CrossRef]

28. Ali, A.; Qadir, A.; Kuddus, M.; Saxena, P.; Abdin, M.Z. Production of biodiesel from algae: An update. *Handb. Ecomater.* **2019**, *3*, 1953–1964. [CrossRef]

29. Fischer, C.R.; Klein-Marcuschamer, D.; Stephanopoulos, G. Selection and optimization of microbial hosts for biofuels production. *Metab. Eng.* **2008**, *10*, 295–304. [CrossRef]

30. Taleb, A.; Kandilian, R.; Touchard, R.; Montalescot, V.; Rinaldi, T.; Taha, S.; Takache, H.; Marchal, L.; Legrand, J.; Pruvost, J. Screening of freshwater and seawater microalgae strains in fully controlled photobioreactors for biodiesel production. *Bioresour. Technol.* **2016**, *218*, 480–490. [CrossRef] [PubMed]

31. Juárez, Á.B.; Vélez, C.G.; Iñiguez, A.R.; Martínez, D.E.; Rodríguez, M.C.; Vigna, M.S.; De Molina, M.D.C.R. A Parachlorella kessleri (Trebouxiophyceae, Chlorophyta) strain from an extremely acidic geothermal pond in Argentina. *Phycologia* **2011**, *50*, 413–421. [CrossRef]

32. Přibyl, P.; Cepák, V.; Zachleder, V. Production of lipids in 10 strains of chlorella and parachlorella, and enhanced lipid productivity in chlorella vulgaris. *Appl. Microbiol. Biotechnol.* **2012**, *94*, 549–561. [CrossRef]

33. Li, X.; Přibyl, P.; Bišová, K.; Kawano, S.; Cepák, V.; Zachleder, V.; Čížková, M.; Brányiková, I.; Vítová, M. The microalga Parachlorella kessleri—A novel highly efficient lipid producer. *Biotechnol. Bioeng.* **2013**, *110*, 97–107. [CrossRef] [PubMed]

34. Fernandes, B.; Teixeira, J.; Dragone, G.; Vicente, A.A.; Kawano, S.; Bišová, K.; Přibyl, P.; Zachleder, V.; Vítová, M. Relationship between starch and lipid accumulation induced by nutrient depletion and replenishment in the microalga Parachlorella kessleri. *Bioresour. Technol.* **2013**, *144*, 268–274. [CrossRef] [PubMed]

35. Kandilian, R.; Taleb, A.; Heredia, V.; Cogne, G.; Pruvost, J. Effect of light absorption rate and nitrate concentration on TAG accumulation and productivity of Parachlorella kessleri cultures grown in chemostat mode. *Algal Res.* **2019**, *39*, 101442. [CrossRef]

36. Taleb, A.; Legrand, J.; Takache, H.; Taha, S.; Pruvost, J. Investigation of lipid production by nitrogen-starved Parachlorella kessleri under continuous illumination and day/night cycles for biodiesel application. *J. Appl. Phycol.* **2018**, *30*, 761–772. [CrossRef]

37. Janssen, J.H.; Wijffels, R.H.; Barbosa, M.J. Lipid production in nannochloropsis gaditana during nitrogen starvation. *Biology* **2019**, *8*, 5. [CrossRef] [PubMed]

38. Simionato, D.; Block, M.A.; La Rocca, N.; Jouhet, J.; Maréchal, E.; Finazzi, G.; Morosinotto, T. The response of Nannochloropsis gaditana to nitrogen starvation includes de novo biosynthesis of triacylglycerols, a decrease of chloroplast galactolipids, and reorganization of the photosynthetic apparatus. *Eukaryot. Cell* **2013**, *12*, 665–676. [CrossRef]

39. Janssen, J.H.; Lamers, P.P.; de Vos, R.C.; Wijffels, R.H.; Barbosa, M.J. Translocation and de novo synthesis of eicosapentaenoic acid (EPA) during nitrogen starvation in Nannochloropsis gaditana. *Algal Res.* **2019**, *37*, 138–144. [CrossRef]

40. Beacham, T.A.; Bradley, C.; White, D.A.; Bond, P.; Ali, S.T. Lipid productivity and cell wall ultrastructure of six strains of Nannochloropsis: Implications for biofuel production and downstream processing. *Algal Res.* **2014**, *6*, 64–69. [CrossRef]

41. Safi, C.; Cabas Rodriguez, L.; Mulder, W.J.; Engelen-Smit, N.; Spekking, W.; van den Broek, L.A.; Olivieri, G.; Sijtsma, L. Energy consumption and water-soluble protein release by cell wall disruption of Nannochloropsis gaditana. *Bioresour. Technol.* **2017**, *239*, 204–210. [CrossRef]

42. Fábregas, J.; Maseda, A.; Domínguez, A.; Ferreira, M.; Otero, A. Changes in the cell composition of the marine microalga, Nannochloropsis gaditana, during a light:dark cycle. *Biotechnol. Lett.* **2002**, *24*, 1699–1703. [CrossRef]

43. Scholz, M.J.; Weiss, T.L.; Jinkerson, R.E.; Jing, J.; Roth, R.; Goodenough, U.; Posewitz, M.C.; Gerken, H.G. Ultrastructure and composition of the Nannochloropsis gaditana cell wall. *Eukaryot. Cell* **2014**, *13*, 1450–1464. [CrossRef] [PubMed]

44. Lubian, L.M. Nannochloropsis gaditana sp. nov., a new Eustigmatophyceae marina. *Lazaroa* **1982**, *4*, 287–293.

45. Krienitz, L.; Hegewald, E.H.; Hepperle, D.; Huss, V.A.; Rohr, T.; Wolf, M. Phylogenetic relationship of Chlorella and Parachlorella gen. nov. (Chlorophyta, Trebouxiophyceae). *Phycologia* **2004**, *43*, 529–542. [CrossRef]

46. Berges, J.A.; Franklin, D.J.; Harrison, P.J. Evolution of an artificial seawater medium: Improvements in enriched seawater, artificial water over the last two decades. *J. Phycol.* **2001**, *37*, 1138–1145. [CrossRef]

47. Pruvost, J.; Van Vooren, G.; Le Gouic, B.; Couzinet-Mossion, A.; Legrand, J. Systematic investigation of biomass and lipid productivity by microalgae in photobioreactors for biodiesel application. *Bioresour. Technol.* **2011**, *102*, 150–158. [CrossRef] [PubMed]

48. Zinkoné, T.R.; Gifuni, I.; Lavenant, L.; Pruvost, J.; Marchal, L. Bead milling disruption kinetics of microalgae: Process modeling, optimization and application to biomolecules recovery from Chlorella sorokiniana. *Bioresour. Technol.* **2018**, *267*, 458–465. [CrossRef] [PubMed]

49. Pruvost, J.; Cornet, J.F.; Goetz, V.; Legrand, J. Modeling dynamic functioning of rectangular photobioreactors in solar conditions. *AIChE J.* **2011**, *57*, 1947–1960. [CrossRef]

50. Ritchie, R.J. Consistent sets of spectrophotometric chlorophyll equations for acetone, methanol and ethanol solvents. *Photosynth. Res.* **2006**, *89*, 27–41. [CrossRef]

51. Strickland, J.D.H.; Parsons, T.R. *A Practical Handbook of Seawater Analysis*, 2nd ed.; Number 167; Fisheries Research Board of Canada: Ottawa, ON, Canada, 1968; p. 185. [CrossRef]

52. Heath, M.R.; Richardson, K.; Kirboe, T. Optical assessment of phytoplankton nutrient depletion. *J. Plankton Res.* **1990**, *12*, 381–396. [CrossRef]

53. Van Vooren, G.; Le Grand, F.; Legrand, J.; Cuiné, S.; Peltier, G.; Pruvost, J. Investigation of fatty acids accumulation in Nannochloropsis oculata for biodiesel application. *Bioresour. Technol.* **2012**, *124*, 421–432. [CrossRef]

54. DuBois, M.; Gilles, K.A.; Hamilton, J.K.; Rebers, P.A.; Smith, F. Colorimetric Method for Determination of Sugars and Related Substances. *Anal. Chem.* **1956**, *28*, 350–356. [CrossRef]

55. Angles, E.; Jaouen, P.; Pruvost, J.; Marchal, L. Wet lipid extraction from the microalga Nannochloropsis sp.: Disruption, physiological effects and solvent screening. *Algal Res.* **2017**, *21*, 27–34. [CrossRef]

56. Taher, H.; Al-Zuhair, S.; Al-Marzouqi, A.H.; Haik, Y.; Farid, M. Effective extraction of microalgae lipids from wet biomass for biodiesel production. *Biomass Bioenergy* **2014**, *66*, 159–167. [CrossRef]

57. Fukuda, H.; Kondo, A.; Noda, H. Biodiesel fuel production by transesterification of oils. *J. Biosci. Bioeng.* **2001**, *92*, 405–416. [CrossRef]

58. Ashokkumar, V.; Agila, E.; Sivakumar, P.; Salam, Z.; Rengasamy, R.; Ani, F.N. Optimization and characterization of biodiesel production from microalgae Botryococcus grown at semi-continuous system. *Energy Convers. Manag.* **2014**, *88*, 936–946. [CrossRef]

59. Takache, H.; Christophe, G.; Cornet, J.F.; Pruvost, J. Experimental and theoretical assessment of maximum productivities for the microalgae Chlamydomonas reinhardtii in two different geometries of photobioreactors. *Biotechnol. Prog.* **2010**, *26*, 431–440. [CrossRef]

60. Rafay, R.; Uratani, J.M.; Hernandez, H.H.; Rodríguez, J. Growth and Nitrate Uptake in Nannochloropsis gaditana and Tetraselmis chuii Cultures Grown in Sequential Batch Reactors. *Front. Mar. Sci.* **2020**, *7*, 1–9. [CrossRef]

61. Cornet, J.F.; Dussap, C.G.; Dubertret, G. A structured model for simulation of cultures of the cyanobacterium Spirulina platensis in photobioreactors: I. Coupling between light transfer and growth kinetics. *Biotechnol. Bioeng.* **1992**, *40*, 817–825. [CrossRef]

62. Dortch, Q. Effect of growth conditions on accumulation of internal nitrate, ammonium, amino acids, and protein in three marine diatoms. *J. Exp. Mar. Biol. Ecol.* **1982**, *61*, 243–264. [CrossRef]

63. Zhang, Z.; Volkman, J.K. Algaenan structure in the microalga Nannochloropsis oculata characterized from stepwise pyrolysis. *Org. Geochem.* **2017**, *104*, 1–7. [CrossRef]

64. Janssen, J.H.; Spoelder, J.; Koehorst, J.J.; Schaap, P.J.; Wijffels, R.H.; Barbosa, M.J. Time-dependent transcriptome profile of genes involved in triacylglycerol (TAG) and polyunsaturated fatty acid synthesis in Nannochloropsis gaditana during nitrogen starvation. *J. Appl. Phycol.* **2020**. [CrossRef]

65. Yüksel, F.; Yüksel, B. The use of ethanol-gasoline blend as a fuel in an SI engine. *Renew. Energy* **2004**, *29*, 1181–1191. [CrossRef]